

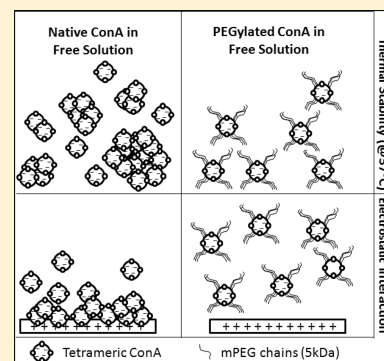
# PEGylation of Concanavalin A to Improve Its Stability for an *In Vivo* Glucose Sensing Assay

Andrea K. Locke,<sup>\*,‡</sup> Brian M. Cummins,<sup>†,‡</sup> Alexander A. Abraham, and Gerard L. Coté

Department of Biomedical Engineering, Texas A&M University, College Station, Texas 77843, United States

**ABSTRACT:** Competitive binding assays utilizing concanavalin A (ConA) have the potential to be the basis of improved continuous glucose monitoring devices. However, the efficacy and lifetime of these assays have been limited, in part, by ConA's instability due to its thermal denaturation in the physiological environment (37 °C, pH 7.4, 0.15 M NaCl) and its electrostatic interaction with charged molecules or surfaces. These undesirable interactions change the constitution of the assay and the kinetics of its behavior over time, resulting in an unstable glucose response. In this work, poly(ethylene glycol) (PEG) chains are covalently attached to lysine groups on the surface of ConA (i.e., PEGylation) in an attempt to improve its stability in these environments. Dynamic light scattering measurements indicate that PEGylation significantly improved ConA's thermal stability at 37 °C, remaining stable for at least 30 days. Furthermore, after PEGylation, ConA's binding affinity to the fluorescent competing ligand previously designed for the assay was not significantly affected and remained at  $\sim 5.4 \times 10^6 \text{ M}^{-1}$

even after incubation at 37 °C for 30 days. Moreover, PEGylated ConA maintained the ability to track glucose concentrations when implemented within a competitive binding assay system. Finally, PEGylation showed a reduction in electrostatic-induced aggregation of ConA with poly(allylamine), a positively charged polymer, by shielding ConA's charges. These results indicate that PEGylated ConA can overcome the instability issues from thermal denaturation and nonspecific electrostatic binding while maintaining the required sugar-binding characteristics. Therefore, the PEGylation of ConA can overcome major hurdles for ConA-based glucose sensing assays to be used for long-term continuous monitoring applications *in vivo*.



Diabetes mellitus disrupts the regulation of the body's blood glucose levels. It currently affects  $\sim 29.1$  million diagnosed and undiagnosed individuals in the United States and  $\sim 347$  million worldwide.<sup>1,2</sup> Poorly regulated blood glucose levels can lead to serious secondary complications such as kidney failure, heart disease, and blindness.<sup>3</sup> In order to minimize these complications, patients must self-regulate their blood glucose concentrations. This typically involves taking routine blood glucose measurements and making the necessary adjustments to their diet, exercise, and/or medication to maintain euglycemia. In recent years, continuous glucose monitoring (CGM) has been identified as a means to improve diabetes management. Current commercially available CGM devices require frequent calibrations and must be replaced after 3–7 days.<sup>4</sup> Therefore, many research efforts are underway in an attempt to generate improved CGM devices with longer lifetimes and fewer calibrations. One such approach is based on a fluorescent affinity sensor comprised of concanavalin A (ConA).<sup>5–9</sup>

ConA, a lectin extracted from the jack bean, is a tetramer at physiological pH (7.4) comprised of four identical monomeric subunits (MW  $\sim 25$  kDa).<sup>10,11</sup> Each monomer contains an independent carbohydrate binding site, for which glucose and mannose monosaccharides can bind.<sup>12</sup> It has been shown that ConA has the ability to reversibly bind to glucose with an affinity of  $\sim 400 \text{ M}^{-1}$ .<sup>13</sup> This affinity allows the capability for ConA to track physiologically relevant glucose concentrations.

Therefore, ConA is an attractive receptor to be used in a next generation nonenzymatic sensor.

The first noted ConA-based competitive binding assay for glucose sensing was developed by Schultz et al. and employed 70 kDa fluorescein-isothiocyanate dextran (FITC-dextran) as the competing ligand.<sup>14,15</sup> This scheme used a semipermeable membrane to contain the sensing assay and allowed glucose to equilibrate with the external environment. Changing glucose concentrations within the membrane changed the equilibrium binding of assay components, which was transduced into a fluorescent signal that could be measured. Since this introduction, many different variations of the sensing assay have been designed and studied using the same scheme due to its tremendous potential for use in CGM devices.<sup>16–22</sup> Certain assay variations have immobilized ConA to a solid-phase (microdialysis membranes, beads, etc.) while leaving the competing ligand in free solution.<sup>23</sup> This approach has been shown to track glucose concentrations in the body for up to 16 days.<sup>24</sup> Other variations have left both assay components in free solution. Practically, this approach allows the sensor to be developed modularly, where the assay can be developed without requiring the semipermeable membrane. In addition, this approach can potentially minimize the equilibration time to changing glucose concentrations. However, the solution-based

Received: May 13, 2014

Accepted: August 18, 2014

Published: August 18, 2014

approach has shown problems with stability which is a major obstacle in the advancement of the technology for such embedments.<sup>25</sup>

This instability has partly been due to the specific sugar-dependent aggregation seen in assays that pair traditional high-affinity competing ligands (e.g., dextran, glycosylated dendrimer, etc.) with ConA in free solution.<sup>26,27</sup> Since ConA is a tetramer, it presents multiple binding sites that can aggregate with these multivalent competing ligands over time. The resulting lattice-type aggregate eventually precipitates out of solution and requires a significantly higher concentration of glucose to break it apart. This type of instability has recently been addressed by the introduction of a new type of fluorescent competing ligand. This ligand avoids this specific aggregation by presenting a single high affinity moiety for ConA to bind.<sup>28</sup> As a result, the ligand does not present additional residues for ConA to bind once it is already bound, allowing for the assay to remain stable in free solution.

Another aspect of the original assay's instability is associated with ConA's thermal denaturation at physiological temperatures. Since ConA is a protein, it is prone to unfolding, aggregation, and degradation.<sup>29,30</sup> At elevated temperatures, the associated energy can increase the likelihood that the protein unfolds. This unfolding can expose the hydrophobic residues, typically found in the interior of the protein, to the solvent. These residues can interact with neighboring exposed hydrophobic groups leading to aggregation. This aggregation is believed to be irreversible and diminishes the solubility and activity of the protein.<sup>18,31</sup> Vetri et al. have reported that ConA undergoes this denaturation-induced aggregation at  $\sim 40$  °C.<sup>32</sup> Changes in ConA's activity due to aggregation can significantly impact the glucose response of the assay by changing the concentration of active binding sites for which glucose can bind. Therefore, to maximize the *in vivo* lifetime of a ConA-based glucose assay, it is desirable to minimize the rate of ConA's thermal denaturation at physiologically relevant temperatures. The immobilization of ConA to the solid-phase presumably maintains the assay stability by either stabilizing ConA and/or preventing unfolded ConA from aggregating with itself.

In addition to this thermal denaturation, ConA has a tendency to adhere to positively charged surfaces. This electrostatic interaction is due to ConA's overall negative charge under physiological conditions. This is due to its isoelectric point (pI) of  $\sim 5$ , which is defined as the pH at which a particular molecule carries no net electrical charge.<sup>33</sup> This adhesion of ConA to surfaces or molecules can change the concentration and the activity of the receptor in solution. This becomes important when considering encapsulation of the assay for the purpose of *in vivo* implantation. Layer-by-layer (LbL) microcapsules are attractive semipermeable candidates that can be tuned to effectively encapsulate the assay while allowing for the rapid equilibration of smaller analytes with its exterior environment (e.g., glucose). However, proteins have shown the tendency to electrostatically attach to the capsule's inner charged surface.<sup>34</sup> If ConA behaves in a similar manner, the functionality of the assays would be affected as the availability of active receptors within the capsules may decrease. Thus, if LbL microcapsules are to be used, it would be preferable for ConA to avoid undergoing electrostatic interactions with the capsule.<sup>4</sup>

PEGylation is the process by which PEG chains are covalently attached to various molecules and surfaces to improve their stability, solubility, and biocompatibility.<sup>35,36</sup>

The enhanced stability and solubility of a molecule (e.g., protein) via PEG chains is believed to be a result of a hydration barrier created by the grafted hydrophilic chains.<sup>37</sup> In addition, the rapid mobility of the chains provides a steric hindrance effect that may aid in the reduction of particle–particle interaction depending on the chain length.<sup>38</sup> These characteristics of PEG are believed to aid in the reduction of protein aggregation and precipitation. Groups such as Rajan et al., Rodriguez-Martinez et al., and Veronese et al. have shown evidence of this with the attachment of different molecular weight PEG chains to protein molecules such as  $\alpha$ -chymotrypsin and a hematopoietic cytokines.<sup>39–41</sup> Furthermore, Wu et al. have shown an additional advantage of the chains in the role of masking surface charges to minimize nonspecific electrostatic binding of proteins or cells to their imaging contrast agent.<sup>42</sup>

These characteristics have allowed for PEGylation to be used to improve drug delivery systems, reduce protein adhesion, and increase molecular solubility in free solution. In terms of ConA, Kim and Park have shown that the conjugation of PEG chains to ConA increased its solubility at room temperature (22 °C) for the purpose of designing a hydrogel comprised of immobilized ConA for insulin delivery.<sup>43,44</sup> Herein, we investigate the use of PEGylation to minimize the aforementioned nonspecific interactions of ConA to improve the associated stability of the solution-based glucose monitoring approach in a physiologically relevant environment. We show that PEGylation decreases the rate of ConA aggregation with itself at body temperature without significantly affecting the binding affinity to the fluorescent competing ligand and its ability to track physiological glucose concentrations. We also observe that PEGylation reduces the electrostatic interactions between the lectin and positively charged surfaces which may prove to be useful for microencapsulation of the assay for *in vivo* glucose sensing.

## ■ EXPERIMENTAL SECTION

**Materials.** ConA Type IV lyophilized powder, manganese(II) chloride ( $\text{MnCl}_2$ ), Trizma hydrochloride (Trizma-HCl), sodium bicarbonate, poly(allylamine) ( $\text{PAH}^+$ ), and methyl- $\alpha$ -D-mannopyranoside (MaM) were purchased from Sigma (St. Louis, MO). Dextrose (D-glucose) was purchased from Fisher Scientific (Hampton, New Hampshire). Methoxyl-poly(ethylene glycol)-N-hydroxylsuccinimide-succinimidyl carbonate (mPEG-NHS (SC), 5 kDa) was purchased from Nanocs (New York, NY). Calcium chloride dihydrates ( $\text{CaCl}_2$ ) and sodium chloride (NaCl) were purchased from Mallinckrodt Chemical Inc. (St. Louis, MO) and J.T. Baker (Center Valley, PA), respectively. Acetone was obtained from Avantor Materials (Center Valley, PA). Fluorescamine was obtained from Life Technologies (Grand Island, NY). The competing ligand, amino-pyrene trisulfonate mannotetraose (APTS-MT), was synthesized with Dr. Vigh at Texas A&M University as previously described.<sup>28</sup> A 0.2  $\mu\text{m}$  syringe filter from VWR (Radnor, PA) was used to filter all solutions before each experiment. All buffers were made using deionized water (DI  $\text{H}_2\text{O}$ ) with a resistance of  $\sim 18$  M $\Omega$  cm, and experiments were performed in TRIS buffer (pH 7.4, 10 mM Trizma-HCl, 0.15 M NaCl, 1 mM  $\text{MnCl}_2$ , and 1 mM  $\text{CaCl}_2$ ) or 0.1 M sodium bicarbonate buffer (pH 8.5 and 0.15 M NaCl).

**PEGylation of ConA.** ConA was PEGylated with 5 kDa mPEG-NHS (SC), a primary amine reactive polymer that contains a succinimidyl carbonate linker. Briefly, ConA was

dissolved in sodium bicarbonate buffer (10 mg mL<sup>-1</sup>). The solution's peak absorbance at ~280 nm was measured using a Hitachi U-4100 UV-vis-NIR spectrophotometer (Hitachi High Technologies American Inc., U.S.) to determine the concentration of the solution using an extinction coefficient of 118 560 M<sup>-1</sup> cm<sup>-1</sup> based on the  $E^{1\%}$  of 11.4 and MW of ~104 kDa.<sup>45</sup> A highly concentrated aliquot of MaM was added to the ConA solution for a final MaM concentration of 1.9 mg mL<sup>-1</sup> in an attempt to protect the activity of the binding sites of ConA during the reaction. Next, mPEG-NHS (SC) was added at a molar ratio of 16:1 to the ConA monomer. At 22 °C, this solution was mixed on a rotating wheel for 6 h and then allowed to continue reacting for 18 h without mixing. The solution was subsequently separated into two dialysis tubes (MWCO 20 kDa). One tube was dialyzed against sodium bicarbonate buffer for PEGylation characterization with fluorescamine, while the remaining solution was dialyzed against TRIS buffer for all other experiments. Following dialysis, absorption measurements were again performed to determine the final PEGylated ConA concentrations, using the same molar extinction coefficient as unmodified ConA.

**PEGylation Characterization.** The average degree of PEGylation was estimated using fluorescamine, as it is a useful tool to track the concentration of primary amines within a solution.<sup>46</sup> Fluorescamine becomes fluorescent after reacting with primary amines, and changes in fluorescence intensity can be descriptive of the makeup of the solution. This was used to compare identical concentrations of unmodified and PEGylated ConA to determine their relative concentrations of primary amines. This difference is related to the approximate number of mPEG chains grafted per ConA monomer.

Briefly, a range of concentrations of unmodified ConA and PEGylated ConA (0–2.5 μM) were prepared in sodium bicarbonate buffer (1.5 mL). Then, 500 μL of fluorescamine (0.3 mg mL<sup>-1</sup> in acetone) was added to each solution and mixed well. Subsequently, 100 μL of each solution was added to a standard black 96-well microplate. After 5 min, the fluorescence intensity of each solution was measured using a TECAN Infinite 200 PRO microplate reader (Tecan Group Ltd., Männedorf, Switzerland) at  $\lambda_{\text{ex}} = 390$  nm and  $\lambda_{\text{em}} = 475$  nm. These fluorescence intensities were plotted against the corresponding ConA concentrations, and the linear regression was performed to obtain the slopes,  $m_{\text{mPEG-ConA}}$  and  $m_{\text{ConA}}$ . These slopes were used in eq 1 to estimate the average degree of PEGylation (DP), similar to Wen et al.<sup>47</sup>

$$\text{DP} = \left( 1 - \frac{m_{\text{mPEG-ConA}}}{m_{\text{ConA}}} \right) \times 13 \quad (1)$$

This equation was utilized under the assumptions that fluorescamine could originally interact with each of the primary amines on unmodified ConA and that it could interact with each of the primary amines that remained on PEGylated ConA. Therefore, the differences in the fluorescence intensities are assumed to be solely due to the decrease in the primary amine concentration resulting from the conjugated PEG chains.

**Thermal Stability.** The thermal denaturation of unmodified and PEGylated ConA in free solution was tracked by monitoring the aggregation in a physiologically relevant buffer with dynamic light scattering (DLS). In sealed disposable polystyrene cuvettes (1 cm path length), solutions of unmodified and PEGylated ConA (10 μM each) were prepared in triplicate in TRIS buffer. The cuvettes were incubated at 37

°C. Over the course of 30 days, measurements were taken at seven different time points (days 0, 1, 2, 4, 9, 16, and 30) with resuspension of the particles via aspiration before each measurement. A Malvern Nano Zetasizer (Malvern Instruments Ltd., Worcestershire, U.K.) was used to measure the average particle diameter (Z-average) as well as the polydispersity index (PDI) of the particles within each solution.

**Binding Affinity.** The binding affinity of unmodified and PEGylated ConA to the rationally designed fluorescent competing ligand, APTS-MT, was evaluated using fluorescence anisotropy. In the wells of a standard black 96-well microplate, solutions were prepared with a fixed concentration of APTS-MT (100 nM) and a range of concentrations of either unmodified or PEGylated ConA (4 nM to 10 μM). Solutions were prepared in TRIS buffer, and each well had a final volume of 100 μL. The appropriate controls (TRIS buffer and 100 nM APTS-MT) were also added to separate microplate wells for baseline correction purposes. Time was then given for all solutions to reach equilibrium (~10 min) at 22 °C, and a TECAN Infinite F200 microplate reader fitted with polarizers was used to measure the steady-state fluorescence anisotropy of each solution ( $\lambda_{\text{ex}} = 483$  nm;  $\lambda_{\text{em}} = 540$  nm). The affinity was determined by plotting the average anisotropy as a function of the tetrameric ConA concentration on a logarithmic scale and fitting the data with a Boltzmann curve.

To determine the stability of this binding in a physiologically relevant environment, the stock solution of PEGylated ConA was then stored at 37 °C for 30 days. Portions of this stock solution were withdrawn at various time points during this period (days 1, 2, 4, 9, 16, and 30) and tested via fluorescence anisotropy in the same manner.

**Glucose Response.** PEGylated ConA was tested using a fluorescence anisotropy assay comprised of 200 nM APTS-MT (the competing ligand) and 1 μM PEGylated ConA to determine its effectiveness in tracking physiological glucose concentrations. Various concentrations of D-glucose (0 to ~800 mg dL<sup>-1</sup>) were prepared in TRIS buffer and verified using a YSI 2300 Stat Plus biochemistry analyzer. A stock assay containing 2 μM mPEG-ConA and 400 nM APTS-MT was prepared in TRIS buffer. In a standard black 96-well microplate, 50 μL of the assay and 50 μL of the appropriate glucose concentrations were added to separate wells and a mixed well. This created wells containing a final assay concentration of 200 nM APTS-MT and 1 μM PEGylated ConA with glucose concentrations ranging from 0 to ~400 mg dL<sup>-1</sup>. Like before, the appropriate controls (TRIS buffer and 200 nM APTS-MT) were also added to separate microplate wells for baseline correction purposes. After time was given for the solutions to equilibrate (~10 min) at 22 °C, the steady-state anisotropy of each solution was measured with the TECAN Infinite F200 microplate reader.

**Nonspecific Adsorption.** Light scatter can be used to investigate the interaction of macromolecules in free solution, including those containing proteins. For example, Park et al. have used this method to study the electrostatic interaction between different biological proteins (i.e., BSA, RNase, and lysozymes) and polyelectrolytes (i.e., PSS, PVS, etc.) via turbidity measurements at 420 nm.<sup>48</sup> This turbidity is related to the amount of aggregation within the various samples and is indicative of the specific and/or nonspecific binding between molecules.

In a similar manner, the electrostatic interactions of PAH<sup>+</sup> (a common polyelectrolyte used in LbL) with unmodified and PEGylated ConA was measured in this study. In separate



centrifuge tubes, each of the following solutions was prepared in triplicate in TRIS buffer at 22 °C: PAH<sup>+</sup> with ConA, PAH<sup>+</sup> with PEGylated ConA, ConA, PEGylated ConA, and PAH<sup>+</sup>. Each individual component in each solution was prepared at 10  $\mu$ M for comparison. Immediately after preparation, 100  $\mu$ L of each sample was extracted and added to a standard UV–vis 96-well microplate. The turbidity of each solution was then measured at 400 nm using a TECAN Infinite 200 PRO microplate reader. These measurements were also performed at 30 min, 1 h, 24 h, and 48 h.

## RESULTS AND DISCUSSION

**Degree of PEGylation.** Each ConA monomer contains 13 primary amines that can potentially be PEGylated (12 lysine residues and the N-terminus).<sup>43</sup> Figure 1 shows that fluoresc-

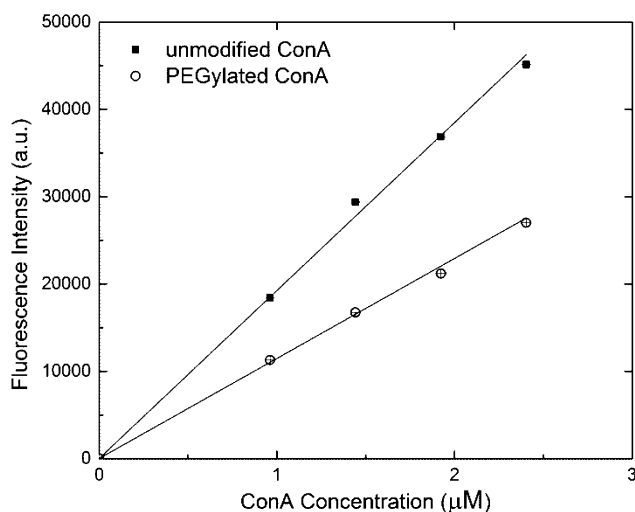


**Figure 1.** Decrease in the fluorescence intensity of fluorescamine in the presence of PEGylated ConA compared to unmodified ConA, indicating the degree of PEGylation.

amine's fluorescence intensity was consistently lower in solutions of PEGylated ConA than it was for unmodified ConA at the same concentration. This indicates that the presence of the mPEG chains decreased the interaction between fluorescamine and the primary amines on the PEGylated ConA. Equation 1 estimates an average of  $\sim 5.36$  mPEG chains grafted per ConA monomer. Assuming a Poisson distribution, this degree of PEGylation would mean that 99.9% of ConA tetramers have 8 or more mPEG chains per tetramer. While the average number of mPEG chains grafted per ConA could be lower than the estimated value from eq 1, the PEGylated ConA is expected to be sufficiently modified for the purpose of this study.

**Thermal Stability.** The thermal stability of unmodified and PEGylated ConA was investigated by tracking the time dependent aggregation of the protein within the solutions at 37 °C. Per Figure 2, the average particle size in the unmodified ConA solution displayed an initial (i.e., day 0) diameter of  $8 \pm 0.03$  nm, consistent with previous reports for the hydrodynamic diameter of unmodified tetrameric ConA.<sup>49</sup> The average particle size in the PEGylated ConA solution displayed a higher initial diameter of  $30 \pm 0.22$  nm (Figure 2), due to the increase in the aforementioned hydration barrier associated with multiple mPEG chains.

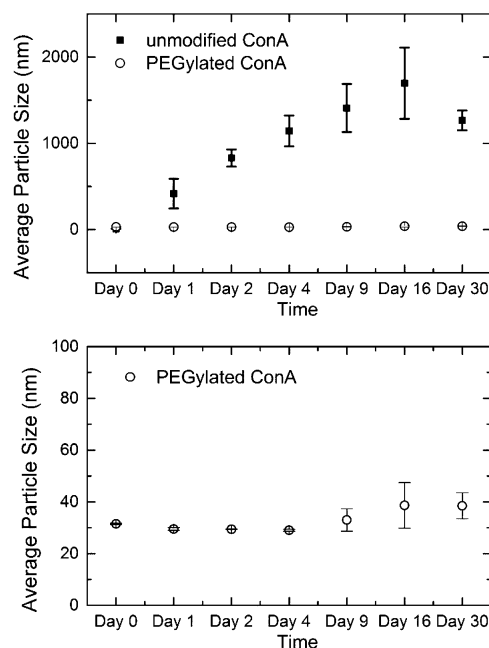


**Figure 2.** Z-average particle size of unmodified ConA compared to PEGylated ConA (top) in response to incubation at 37 °C, over the course of 30 days. In the bottom panel, PEGylated ConA is rescaled to show its average particle size. The error bars show the standard deviation for three different runs.

After 24 h, the average diameter of particles in the unmodified ConA solution increased to over 400 nm. After 30 days at 37 °C, the average diameter of particles in the solution of unmodified ConA increased to  $\sim 1.8$   $\mu$ m (Figure 2), indicating aggregation of the ConA molecules. The slight decrease in particle size for unmodified ConA between day 16 and day 30 is believed to be due to the precipitation of the larger aggregates during the measurements. Overall, this type of aggregation clearly indicates that unmodified ConA is thermally unstable in this environment.

In contrast, Figure 2 shows that the average particle size in the PEGylated ConA solution remained relatively constant at  $\sim 30$ – $38$  nm over 30 days at 37 °C. This indicates that PEGylated ConA displays negligible thermally induced aggregation and suggests that ConA's thermal stability has indeed been improved via this degree of PEGylation. The slight increase in standard error of the average size of PEGylated ConA could be due to the small percentage of ConA molecules that displays either low levels of PEGylation or no PEGylation at all. Without sufficient PEGylation, this population is expected to display properties similar to that of unmodified ConA. Strategies could potentially be employed to remove this small percentage prior to the use of PEGylated ConA in a sensor.

The polydispersity of the particle sizes within a solution can also be used to describe that solution. For instance, aggregation is expected to produce a large distribution of particle sizes, which would display a high level of polydispersity. For the DLS measurements reported here, the polydispersity index (PDI) indicates the level of polydispersity and ranges from 0 (low dispersity) to 1 (completely disperse).

Figure 3 shows the comparison of time-dependent PDI of the solutions for unmodified and PEGylated ConA at 37 °C. Initially, the PDI of the PEGylated ConA is slightly higher than

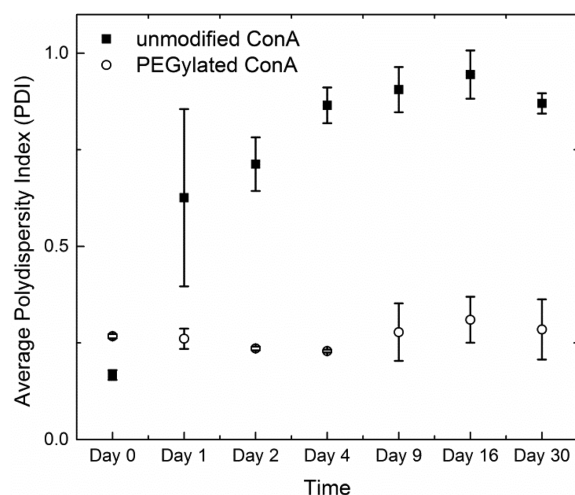


**Figure 3.** Average PDI of unmodified and PEGylated ConA at 37 °C for 30 days. The error bars show the standard deviation for three different runs.

the unmodified ConA. This is presumably due to the range of degrees of PEGylation that is to be expected with a Poisson distribution. However, over the course of the 30 days of this experiment, the PDI of the unmodified ConA solution increased from 0.2 to 0.87 implying that the solutions of unmodified ConA became increasingly heterogeneous as the formation of aggregates increased (Figure 3). In comparison, Figure 3 shows that PEGylated ConA remained relatively homogeneous in solution over the same time period. This result confirms what was observed in Figure 2; the average particle size of PEGylated ConA remains relatively constant and does not aggregate. These characteristics suggest that this degree of PEGylation improves the thermal stability of ConA at physiological conditions. It is important to note that this improved stability could be due to an inhibition of the aggregation of unfolded ConA via steric hindrance, an improved conformational stability of ConA, or a combination thereof.

**Binding Affinity.** While PEGylation does increase the thermal stability of ConA, the PEGylated protein must maintain its binding capability to be functional in a competitive binding assay. The degree to which ConA's binding is affected by PEGylation is likely to be dependent on the chain length and the number of chains grafted. However, for a given degree of PEGylation, it is expected to have a greater effect on the binding of the competing ligand than that of glucose due to relative size. Therefore, ConA's binding to the fluorescent competing ligand (APTS-MT) of the competitive binding assay was investigated. For PEGylated ConA to be used in a competitive binding assay and optimally track physiological glucose concentrations, an affinity of  $10^5$  to  $10^7$   $M^{-1}$  to the competing ligand is required.<sup>28</sup> Binding studies would need to be performed if a different competing ligand or degree of PEGylation were to be used. In addition, if a traditional competing ligand is used, additional experiments should be performed to determine whether sugar-dependent aggregation is occurring. This is because PEGylation of ConA could avoid the aggregation with such ligands through steric hindrance effects.

Herein, the binding affinity ( $K_a$ ) of APTS-MT to unmodified and PEGylated ConA was evaluated using fluorescence anisotropy. Fluorescence anisotropy is a useful tool that can

provide information about protein–ligand interactions. Briefly, polarized light is used to selectively excite a portion of the fluorescent ligand within solution. The average rotational diffusion of the molecules at equilibrium can be tracked with the polarization of the fluorescence. This fluorescence polarization/anisotropy increases as the binding of the fluorescent ligand to the desired protein increases.<sup>50</sup> The parallel and perpendicular components of the fluorescent emission can be measured, and the fluorescence anisotropy can be calculated with eq 2.<sup>51</sup>

$$r = \frac{I_{vv} - (I_{vh}G)}{I_{vv} + (2I_{vh}G)} \quad (2)$$

In this equation,  $r$  is the anisotropy,  $G$  is the correction factor due to the instrument's sensitivity or biased to one polarizer over the other, and  $I_{vv}$  and  $I_{vh}$  are the vertically and horizontally polarized fluorescence intensities, respectively. The dissociation constant ( $K_d$ ) was determined from a plot of the anisotropy as a function of varying ConA concentration using a Boltzmann curve fit.

The association constants ( $K_a$ ) for unmodified and PEGylated ConA were  $\sim 5.7 \pm 0.37 \times 10^6$   $M^{-1}$  and  $\sim 5.4 \pm 0.37 \times 10^6$   $M^{-1}$ , respectively. Therefore, PEGylation did not significantly affect the binding affinity of ConA to the competing ligand. Moreover, PEGylated ConA's affinity falls within the range necessary for this assay to be optimized across physiological glucose concentrations.

In addition, the capability of PEGylated ConA to maintain its binding affinity after incubation at 37 °C was evaluated. Since anisotropy is sensitive to scatter, measurements of unmodified ConA were not possible due to the large aggregate formation similar to those observed during the thermal studies.

Figure 4 indicates that the binding affinity of PEGylated ConA to the competing ligand remained stable at  $\sim 5.4 \pm 0.5 \times$

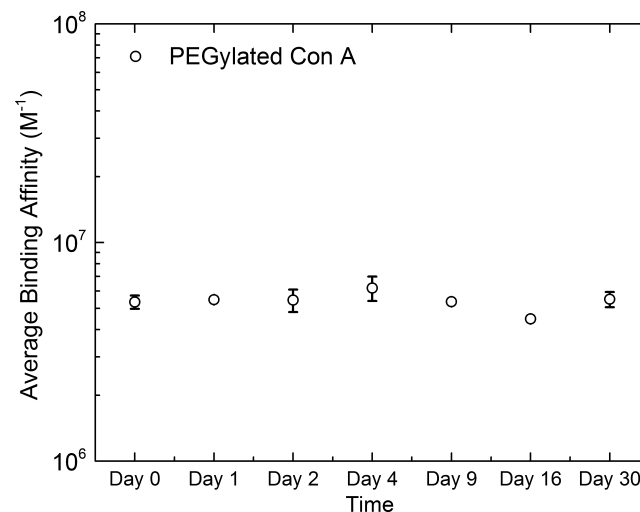


**Figure 4.** Stability of the binding affinity of PEGylated ConA to the competing ligand. The error bars show the standard deviation for three different runs.

$10^6$   $M^{-1}$  over 30 days. The slight fluctuations in affinity may be related to pipet error during mixing and sample transfer from the cuvette to the microplate. This result, along with its thermal stability in free solution, suggests that the activity of ConA can be maintained via PEGylation which may allow for long-term functionality of a ConA-based sensor. Furthermore, because

ConA's binding is due to its folded structure, the long-term binding stability suggests that the protein maintains its functional conformation over time. Therefore, we expect that PEGylation is most likely enhancing ConA's conformational stability in addition to any steric-hindrance effects that it also imparts.

**Glucose Response.** PEGylated ConA was expected to maintain its response to glucose because the binding of APTS-MT was not hindered by the presence of the PEG chains (Figure 4) and glucose (MW ~180 Da) is smaller than APTS-MT (MW ~1 kDa). To verify this, fluorescence anisotropy was used to track the behavior of an assay comprised of PEGylated ConA and APTS-MT in the presence of varying concentrations of glucose (Figure 5). This displays a characteristic competitive

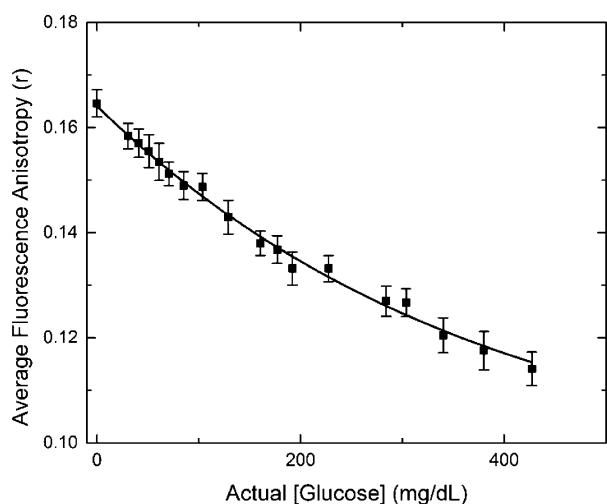


**Figure 5.** Glucose response of fluorescence anisotropy assay using PEGylated ConA (1  $\mu$ M PEGylated ConA and 200 nM APTS-MT). Solid line: best fit to experimental data using the competitive binding equation. The error bars show the standard deviation for three different runs.

binding curve, where the anisotropy decreases in response to increasing glucose concentrations. This indicates that the PEGylation of ConA does not inhibit its ability to track physiological glucose concentrations in the competitive binding assay.

**Nonspecific Adsorption.** The effect that PEGylation had on the electrostatic interactions between ConA and positively charged molecules was studied using PAH<sup>+</sup>. Unmodified and PEGylated ConA were allowed to interact with PAH<sup>+</sup> in free solution, and turbidity measurements at 400 nm were used to evaluate aggregation. ConA absorbs ultraviolet light with a peak at ~280 nm and absorbs a negligible amount of light above ~320 nm. Therefore, any extinction of the incident light higher than 320 nm is assumed to be scattered light that is associated with aggregate formation within the solution.

The electrostatic-induced aggregation between the negatively charged unmodified ConA and the positively charged PAH<sup>+</sup> is observed with the increase in scatter in comparison to its control, unmodified ConA without PAH<sup>+</sup> (Figure 6). Moreover, the unmodified ConA/PAH<sup>+</sup> aggregates were observed as white particulates within the solution (Figure 7). In contrast, PEGylated ConA's interaction with PAH<sup>+</sup> showed relatively no change in scattering, indicating no aggregate formation. This may be due to the masking of the charges on ConA by the

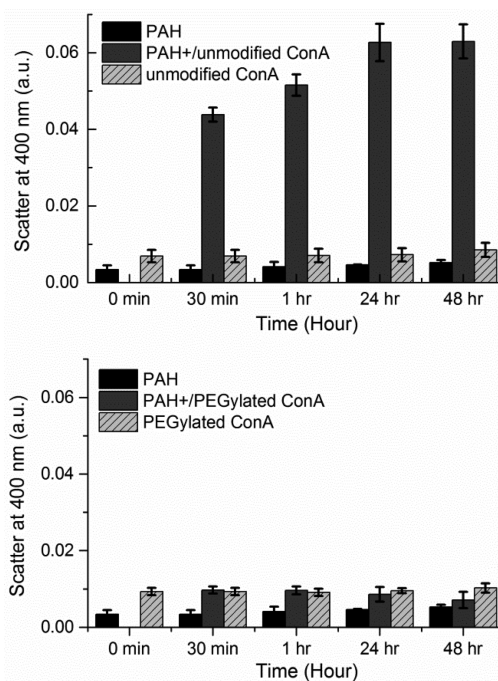


**Figure 6.** Scattering effect due electrostatic interaction between unmodified ConA (top) and PEGylated ConA (bottom) with PAH<sup>+</sup>. The error bars show the standard deviation for three different runs.

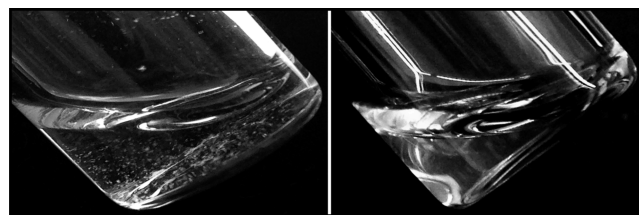


**Figure 7.** Aggregate formation ("white particulate") during unmodified ConA/PAH<sup>+</sup> electrostatic interaction (left) versus PEGylated ConA/PAH<sup>+</sup> (right).

mPEG chains and thereby preventing ConA adhesion to PAH<sup>+</sup>. To validate this data, separate solutions of ConA, PEGylated ConA, and PAH<sup>+</sup> were used as controls. During the same time period, there were no changes in the scatter of these controls. This establishes that the increase in scatter was a direct result of the interaction between unmodified ConA and PAH<sup>+</sup>. Therefore, PEGylation proved useful in the minimization of electrostatic-induced aggregation of ConA. This is desirable when aiming to encapsulate the ConA based assay within a carrier (e.g., layer-by-layer microcapsules) as it may allow the assay to remain free in solution and, thus, maintain its full activity.

## CONCLUSIONS

ConA was modified via PEGylation in an attempt to overcome major obstacles associated with its translation to *in vivo* applications. While unmodified ConA showed immediate instability in free solution within a physiologically relevant environment, PEGylated ConA showed no such aggregation for at least 30 days. This stability in free solution allowed for its binding affinity to be tested over the same time period. Results showed that PEGylated ConA maintains an ideal binding affinity to the rationally designed APTS-MT for use in a



competitive binding assay, and this utility was displayed by tracking physiologically relevant glucose concentrations using a fluorescence anisotropy assay. Moreover, PEGylated ConA is capable of resisting electrostatic interactions with PAH<sup>+</sup>, a polymer typically used in layer-by-layer encapsulation strategies. Together, these results with PEGylated ConA are encouraging for the development of a ConA-based continuous glucose monitoring device for *in vivo* application.

## AUTHOR INFORMATION

### Corresponding Author

\*E-mail: andrealocke88@tamu.edu.

### Present Address

†B.M.C.: North Carolina State University—University of North Carolina, Joint Department of Biomedical Engineering, Raleigh, NC, 27695.

### Author Contributions

‡A.K.L. and B.M.C. contributed equally to this work.

### Notes

The authors declare no competing financial interest.

## ACKNOWLEDGMENTS

The research reported in this publication was supported by the National Institute of Health under the award number R01DK095101. The content is solely the responsibility of the authors and does not necessarily represent the official views of the National Institutes of Health. The authors would like to thank Dr. Melissa Grunlan, Associate Professor of Biomedical Engineering, Texas A&M University, for her expertise and for reviewing this manuscript. They also thank Dr. Michael McShane, Professor of Biomedical Engineering at Texas A&M University, for the use of his microplate reader and the TAMU Materials Characterization Facility for their spectrophotometer.

## REFERENCES

- (1) Centers for Disease Control and Prevention. <http://www.cdc.gov/diabetes/pubs/statsreport14.htm> (accessed August 4, 2014).
- (2) World Health Organization. <http://www.who.int/mediacentre/factsheets/fs312/en/> (accessed August 4, 2014).
- (3) American Diabetes Association. *Diabetes Care* **2011**, *34*, S62.
- (4) Damiano, E. R.; El-Khatib, F. H.; Zheng, H.; Nathan, D. M.; Russell, S. J. *Diabetes Care* **2013**, *36*, 251–259.
- (5) Ballerstadt, R.; Schultz, J. S. *Anal. Chem.* **2000**, *72*, 4185.
- (6) Cummins, B. M.; Lim, J.; Simanek, E. E.; Pishko, M. V.; Coté, G. L. *Biomed. Opt. Express* **2011**, *2*, 1243.
- (7) Ibey, B. L.; Beier, H. T.; Rounds, R. M.; Coté, G. L.; Yadavalli, V. K.; Pishko, M. V. *Anal. Chem.* **2005**, *77*, 7039.
- (8) Russell, R. J.; Pishko, M. V.; Gefrides, C. C.; McShane, M. J.; Cote, G. L. *Anal. Chem.* **1999**, *71*, 3126.
- (9) Sato, K.; Anzai, J.-i. *Anal. Bioanal. Chem.* **2006**, *384*, 1297.
- (10) Hardman, K. D.; Ainsworth, C. F. *Biochemistry* **1972**, *11*, 4910.
- (11) Hardman, K. D.; Ainsworth, C. F. *Biochemistry* **1973**, *12*, 4442.
- (12) Goldstein, I. J.; Hollerman, C. E.; Smith, E. E. *Biochemistry* **1965**, *4*, 876.
- (13) Mandai, D. K.; Brewer, C. F. *Biochemistry* **1993**, *32*, 5116.
- (14) Schultz, J. S.; Mansouri, S.; Goldstein, I. J. *Diabetes Care* **1982**, *5*, 245.
- (15) Schultz, J. S.; Sims, G. *Biotechnol. Bioeng. Symp.* **1979**, No. 9, 65.
- (16) Aloraefy, M.; Pfefer, J.; Ramella-Roman, J.; Sapsford, K. *Proceedings of SPIE*, 2012, 8367, 8367OH.
- (17) Ballerstadt, R.; Evans, C.; McNichols, R.; Gowda, A. *Biosens. Bioelectron.* **2006**, *22*, 275.
- (18) Ballerstadt, R.; Polak, A.; Beuhler, A.; Frye, J. *Biosens. Bioelectron.* **2004**, *19*, 905.
- (19) Meadows, D.; Schultz, J. S. *Talanta* **1988**, *35*, 145.
- (20) Meadows, D. L.; Schultz, J. S. *Anal. Chim. Acta* **1993**, *280*, 21.
- (21) Peng, J.; Wang, Y.; Wang, J.; Zhou, X.; Liu, Z. *Biosens. Bioelectron.* **2011**, *28*, 414.
- (22) Pickup, J. C.; Hussain, F.; Evans, N. D.; Sachedina, N. *Biosens. Bioelectron.* **2005**, *20*, 1897.
- (23) Srinivasan, K. R.; Mansouri, S.; Schultz, J. S. *Biotechnol. Bioeng.* **1986**, *28*, 233.
- (24) Ballerstadt, R.; Evans, C.; Gowda, A.; McNichols, R. *Diabetes Technol. Ther.* **2006**, *8*, 296.
- (25) Cummins, B. M.; Garza, J. T.; Coté, G. L. *Proceedings of SPIE*, 2013, 8591, 859103-6.
- (26) McCartney, L. J.; Pickup, J. C.; Rolinski, O. J.; Birch, D. J. S. *Anal. Biochem.* **2001**, *292*, 216.
- (27) Tolosa, L.; Malak, H.; Raob, G.; Lakowicz, J. R. *Sens. Actuators, B* **1997**, *45*, 93–99.
- (28) Cummins, B. M.; Li, M.; Locke, A. K.; Birch, D. J. S.; Vigh, G.; Coté, G. L. *Biosens. Bioelectron.* **2015**, *63*, 53.
- (29) Huet, C.; Lonchamp, M.; Huet, M.; Bernadac, A. *Biochim. Biophys. Acta, Protein Struct.* **1974**, *365*, 28–39.
- (30) Wang, W. *Int. J. Pharm.* **1999**, *185*, 129–188.
- (31) McKenzie, G. H.; Sawyer, W. H.; Nichol, L. W. *Biochim. Biophys. Acta, Protein Struct.* **1972**, *263*, 283–293.
- (32) Vetri, V.; Canale, C.; Relini, A.; Librizzi, F.; Militello, V.; Gliozzi, A.; Leone, M. *Biophys. Chem.* **2007**, *125*, 184–190.
- (33) Entlicher, G.; Košťář, J. V.; Kocourek, J. *Biochim. Biophys. Acta, Protein Struct.* **1971**, *236*, 795–797.
- (34) Stein, E. W.; Volodkin, D. V.; McShane, M. J.; Sukhorukov, G. B. *Biomacromolecules* **2006**, *7*, 710–719.
- (35) Roberts, M. J.; Bentley, M. D.; Harris, J. M. *Adv. Drug Delivery Rev.* **2002**, *54*, 459–476.
- (36) Veronese, F. M.; Pasut, G. *Drug Discovery Today* **2005**, *10*, 1451–1458.
- (37) Bhat, R.; Timasheff, S. N. *Protein Sci.* **1992**, *1*, 1133–1143.
- (38) Sharma, S.; Popat, K. C.; Desai, T. A. *Langmuir* **2002**, *18*, 8728.
- (39) Rajan, R. S.; Li, T.; Aras, M.; Sloey, C.; Sutherland, W.; Arai, H.; Briddell, R.; Kinstler, O.; Lueras, A. M. K.; Zhang, Y.; Yeghnazar, H.; Treuheit, M.; Brems, D. N. *Protein Sci.* **2006**, *15*, 1063.
- (40) Veronese, F. M.; Mero, A.; Pasut, G. Protein PEGylation, basic science and biological applications. In *PEGylated Protein Drugs: Basic Science and Clinical Applications*; Birkhäuser Verlag: Basel, Switzerland, 2009; pp 11–31.
- (41) Rodríguez-Martínez, J. A.; Solá, R. J.; Castillo, B.; Cintrón-Colón, H. R.; Rivera-Rivera, I.; Barletta, G.; Griebenow, K. *Biotechnol. Bioeng.* **2008**, *101*, 1142.
- (42) Wu, S.-C.; Lin, K.-L.; Wang, T.-P.; Tzou, S.-C.; Singh, G.; Chen, M.-H.; Cheng, T.-L.; Chen, C.-Y.; Liu, G.-C.; Lee, T.-W.; Hu, S.-H.; Wang, Y.-M. *Biomaterials* **2013**, *34*, 4118.
- (43) Kim, J. J.; Park, K. *Pharm. Res.* **2001**, *18*, 794.
- (44) Kim, J. J.; Park, K. *J. Controlled Release* **2001**, *77*, 39.
- (45) Agrawal, B. B. L.; Goldstein, I. J. *Arch. Biochem. Biophys.* **1968**, *124*, 218–229.
- (46) Stocks, S. J.; Jones, A. J. M.; Ramey, C. W.; Brooks, D. E. *Anal. Biochem.* **1986**, *154*, 232–234.
- (47) Wen, Z.; Niemeyer, B. J. *Chromatogr., B* **2011**, *879*, 1732–1740.
- (48) Park, J. M.; Muhoberac, B. B.; Dubin, P. L.; Xia, J. *Macromolecules* **1992**, *25*, 290–295.
- (49) Hardman, K. D.; Wood, M. K.; Schiffer, M.; Edmundson, A. B.; Ainsworth, C. F. *Proc. Natl. Acad. Sci. U.S.A.* **1971**, *68*, 1393–1397.
- (50) Jameson, D. M.; Ross, J. A. *Chem. Rev.* **2010**, *110*, 2685–2708.
- (51) Jameson, D. M.; Sawyer, W. H. *Biochem. Spectrosc.* **1995**, *246*, 283–300.